Materials Research Express

PAPER

Superconductor $YBa_2Cu_{3-x}Ni_xO_{7-\delta}$ compounds prepared by electrospinning

Materials Research Express

PAPER

Superconductor $YBa_2Cu_{3-x}Ni_xO_{7-\delta}$ compounds prepared by electrospinning

RECEIVED
15 February 2019

REVISED
21 April 2019

ACCEPTED FOR PUBLICATION
7 May 2019

PUBLISHED
24 May 2019

J C Bernardi[1], D A Modesto[1], M S Medina[1], A Zenatti[1], E C Venâncio[1], E R Leite[2], A J C Lanfredi[1] and M T Escote[1]

[1] Centro de Engenharia, Modelagem e Ciências Sociais Aplicadas, UFABC, Av. dos Estados 5001, Santo André, SP, 09210-580, Brazil
[2] Laboratório Interdisciplinar de Eletroquímica e Cerâmica, Departamento de Quimica, UFSCAR, Rodovia Washington Luís, Km 235, 13565-905 , São Carlos, SP, Brazil

E-mail: juliane.bernardi@ufabc.edu.br

Keywords: electrospinning, superconductor, perovskite

Abstract

This work describes the synthesis and characterization of $YBa_2Cu_{3-x}Ni_xO_{7-\delta}$ ($0.00 \leqslant x \leqslant 0.04$) compounds prepared by an electrospinning technique. Stoichiometric solutions of Y-Ba-Cu-Ni were used to electrospin nanowires of these compounds, which were dried and heat-treated at temperatures ranging from 350 °C to 925 °C in an oxygen atmosphere. All samples were characterized by x-ray diffraction (XRD), scanning electron microscopy, and temperature magnetization curves. As prepared and dried at 100 °C, these samples present a nanowire shape with a smooth surface, with external diameters of ~600 nm and a large length (>10 μm). After the heat treatment at 780 °C, all of them maintain their nanowire morphology with a rough surface with external diameters of ~600 nm and length values ranging from 5 to 10 μm. All samples crystallize into the perovskite structure with orthorhombic symmetry (*Pmmm* space group). The most intense Bragg reflections arise from the $YBa_2Cu_{3-x}Ni_xO_{7-\delta}$ phase and low-intensity peaks of additional phases. The temperature dependence of magnetization of these nanowires reveals a diamagnetic transition at temperatures close to the critical temperature, T_c, which is related to the superconductor transition in these compounds. The T_c values range between 70 and 93.2 K for samples with $x = 0.04$ to $x = 0.00$, respectively, where the substitution of Cu with Ni results in a lower T_c.

1. Introduction

Since the discovery of cuprate oxides as high critical temperature (HTC) superconductors in 1986, these oxides have been extensively studied, with numerous reports on practical uses for this material [1, 2]. In the last decade, there has been an effort to produce HTC oxides with various shapes suited to their practical applications, such as long cables and wires [2, 3]. In particular, for several technological implementations, it is desirable to fabricate HTC oxides as long wires that can support a much higher electrical current (x100) than conventional copper wires with an electrical resistance close to zero. Such efforts would broaden the applications of HTC superconductor technology, which is important for increasing the energy efficiency of electrical power transmission systems. In addition, low-dimension and small-size superconductors are also candidates for studying electrical transport in nanoscale systems due to their unique size-and shape-dependent properties [3–5]. Several researchers have sought for the existence of a critical size limit beyond which the superconductivity disappears [3, 6, 7]. However, it should be noted that 1D superconductors show a suppression of superconductivity due to phase-slip processes and lower critical currents [3, 8, 9].

Among the HTC oxides, $YBa_2Cu_3O_{7-\delta}$ (YBCO) compounds have been extensively studied in bulk and thin films [10–13], primarily due to their high superconductor transition temperature ($T_c \sim 92$ K). Moreover, a few works have reported on Cu substitution with other 3d elements with similar ionic radii, such as Ni, Fe and Zn [14–16]. Such substitution promotes a T_c shift toward lower temperatures. With the increase of the dopant content (>1%), this superconductor transition disappears. This effect of the dopant is related to various

mechanisms such as disorder in the oxygen sub-lattice, magnetic pair-breaking scattering, changes in the local symmetry, and electronic localization or band filling [14]. In the YBCO structure, the Cu can be present in two distinct crystallographic sites, the Cu(1) chain and the Cu(2) plane. The dopant atom can occupy one site or can be randomly distributed in both sites. Neutron results have indicated that Zn atoms substitute the Cu in the chain position Cu(1), whereas Ni atoms have a site preference for the plane position Cu(2) [14, 15].

With impressive progress in the synthesis of nanostructured YBCO, it is possible to grow these nanostructures through top-down growth methods using thin films [3, 8–10, 17, 18] and bottom-up processing such as electrospinning and pore-filling template procedures [4, 5, 19, 20]. The top-down process can be controlled to produce very small nanowires, known as nano-bridges, but their properties are strongly dependent on the initial films and patterning process [7]. An alternative process is the electrospinning technique, which is an efficient approach for producing oxides and polymers with long fibers (>10 μm) and micro- and nano-sized diameters [4, 19–21]. To prepare oxide fibers by electrospinning, a mixture of metallic precursors with a polymer is used as the electrospinning precursor solution, and the fiber microstructures can be controlled by different parameters such as the solution viscosity, polymer type, etc [21, 22].

YBCO nanowire fabrication via the electrospinning process is generally performed using different metallic precursors, solvents (water, methanol, and ethanol) and polymer bases [poly(vinyl) alcohol, poly(vinyl) pyrrolidone, poly(acrylic acid)] [4, 19, 20]. This approach produces long polycrystalline YBCO fibers with diameters varying from 50 to 500 nm, which present a characteristic superconductor transition at temperatures below $T_c \approx 90$–92 K. Additionally, a slip-phase mechanism can be determined from the YBCO nanowire transport properties [23].

In this context, we describe the preparation and characterization of superconducting $YBa_2Cu_{3-x}Ni_xO_{7-\delta}$ compounds obtained by an electrospinning process. We used a procedure similar to that described by Duarte *et al* [4] and studied the Ni dopant effect in the YBCO matrix. We also performed a detailed crystalline structure study of these nanostructures. The superconductor properties were evaluated by magnetization investigations.

2. Methods

$YBa_2Cu_{3-x}Ni_xO_{7-\delta}$ (x = 0.00, 0.01, 0.02, and 0.04) nanowires were obtained through the electrospinning technique. This synthesis uses precursor solutions with stoichiometric amounts of Y-Ba-Cu, which were prepared through the dissolution of 20% weight of polyvinylpyrrolidone polymer (PVP, Mw = 1,300.000) in a methanol, acetic and propionic acid solution. Then, stoichiometric amounts of the metallic salts, yttrium acetate, barium acetate, and copper acetate were added to the solution. A few drops of ethylene diamine were added to reach pH ≈ 7. These precursor solutions were stirred and maintained at 70 °C to reduce the solution volume and to adjust its viscosity. The viscosities of these solutions were adjusted to values close to 75 cP, measured using a digital viscometer LVDV-IP (Brookfield). This solution was introduced in a syringe to a homemade electrospinning system, in which fiber samples were produced. The electrospinning system consists of a commercial syringe with a metallic needle and a collector (aluminum foil), both of which were connected to a high voltage source (Ormond Beach, model Es30-0). The solutions were electrospun at a positive voltage of 20 kV, with a needle diameter of 0.6 mm, and a needle-collector distance of ∼10 cm. After the electrospinning process, each sample was dried overnight at 100 °C and observed using optical microscopy to verify the fiber morphology of the samples (not shown). These samples were heat-treated at temperatures varying from 350 °C to 925 °C in an oxygen atmosphere.

Thermal gravimetric analysis and differential thermal analysis (TG/DTA) were performed from room temperature to 1000 °C, with a heating rate of 10 °C min^{-1} in an oxygen atmosphere (STA Nietzsche). The crystalline structure was studied through two diffractometers: (a) x-ray diffraction (D8 Focus Bruker), using Cu-Kα ($\lambda = 1.540\,56$ Å) in the range 20 to 80°, with a step of 0.02° and an exposure time of 2 s; and (b) x-ray diffraction (STADI-P—Stoe), using Mo-Kα ($\lambda = 0.709\,3$ Å), with Ge(111) monochromator, in the range 8 to 50°, step of 0.015° and an exposure time of 150 s. A field emission scanning electron microscope (JEOL, model JMS-6701F) was used to analyze the morphology of the YBCO nanowires. The magnetic properties were measured using a magnetometer [MPMS3 SQUID (superconductor quantum interference device), Quantum Design]; these measurements were acquired by following the zero-field cooling (ZFC) and field cooling (FC) procedures. These measurements were performed from 2 to 300 K with applied magnetic fields varying from 10 to 1000 Oe.

3. Results and discussion

Simultaneous TG and DTA was performed to verify the kinetics of the crystalline phase formation and to verify the crystallization temperature of the $YBa_2Cu_{3-x}Ni_xO_{7-\delta}$ compounds. Figure 1 shows TG/DTA curves for

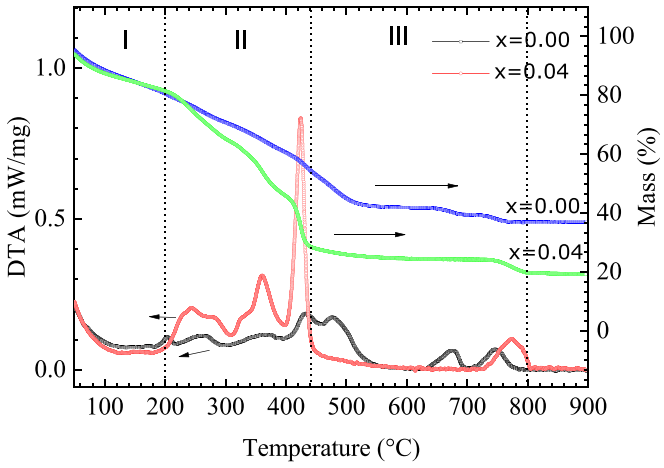

Figure 1. TG/DTA curves of $YBa_2Cu_3O_{7-\delta}$ (YBCO) and $YBa_2Cu_{2.96}Ni_{0.04}O_{7-\delta}$ (YBCNO4) samples electrospun with 75 cP, after drying overnight in a muffle at 100 °C.

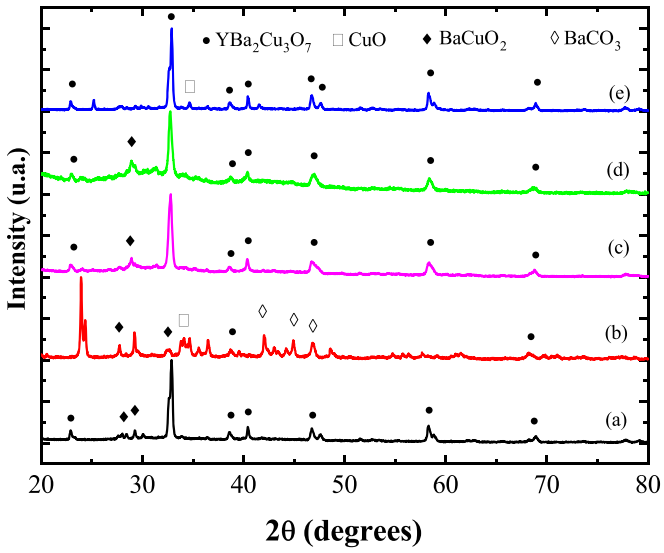

Figure 2. XRD patterns of: (a) $YBa_2Cu_3O_{7-\delta}$ heat treated at 925 °C/4 h; $YBa_2Cu_{3-x}Ni_xO_{7-\delta}$ (x = 0.04) samples heat-treated at (b) 700/4 h °C, (c) 800 °C/4 h; and (d) 925 °C/4 h (radiation Cu-Kα).

$YBa_2Cu_3O_{7-\delta}$ and $YBa_2Cu_{2.96}Ni_{0.04}O_{7-\delta}$ (YBCNO4) samples after they were dried overnight in a furnace at 100 °C. These curves show three main thermal events: (I) Room temperature to 200 °C: weight loss due to the evaporation of some residual water. (II) 200 to 700 °C: weight loss related to the dehydration and evaporation of volatiles. The exothermic peaks in both DTA curves are related to polymer burnout, organic decomposition from the acetates and mixed intermediate phases, as discussed in the literature [4]. (III) Temperatures above 700 °C: the peak and inflexion indicate the beginning of the crystallization process and the formation of the YBCO and doped samples. The results also show a stabilization of weight loss that is compatible with the crystallization process. The temperature of these events changes slightly with the Ni content in the samples; in fact, the crystallization process of the YBCNO4 sample occurs at temperatures above 760 °C. This temperature is lower than the 780 °C observed for the YBCO sample. The heat-treatment conditions were selected based on these results; all samples were calcined at 350 °C and heat-treated at temperatures ranging from 780 to 925 °C in an oxygen atmosphere.

The electrospun samples were submitted to heat treatment at different temperatures and times, which varied from 700 to 925 °C during 4 h to 10 h in an oxygen atmosphere, respectively. This procedure was made in order to reach the desired crystalline structure and to maintain the nanowire shape of these samples. Figure 2 shows x-ray diffraction results for YBCO at 925 °C and the YBCNO4 samples after heat treatment at 700, 780, 800 and 925 °C for 4 to 10 h in an oxygen atmosphere. The XRD patterns of these samples after heat treatment from 700 to 800 °C show the presence of the main Bragg reflection from $YBa_2Cu_3O_{7-\delta}$ (JCPDF 64-642); additional peaks

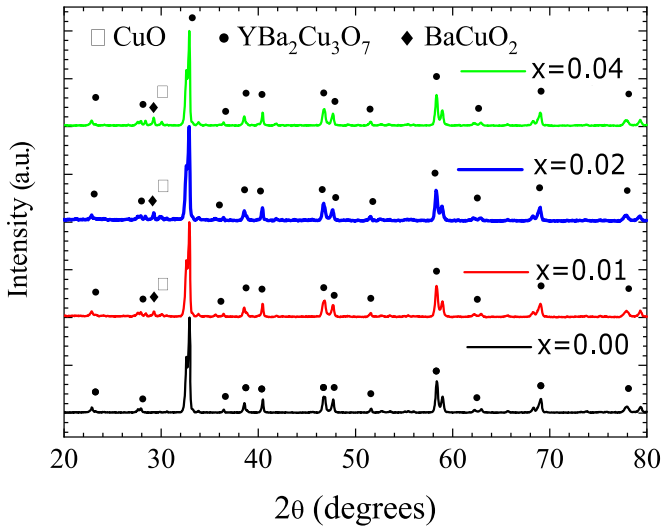

Figure 3. XRD results of $YBa_2Cu_{3-x}Ni_xO_{7-\delta}$ (x = 0.00, 0.01, 0.02 and 0.04) samples heat-treated at 925 °C/4 h in O_2 (radiation Cu-Kα).

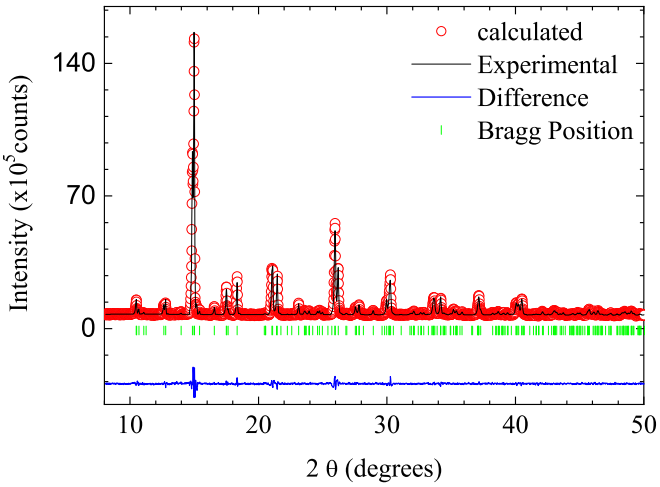

Figure 4. XRD pattern of a YBCO sample and FullProf refinements: (black line) experimental curve, (red dots) theoretical curve, (blue line) difference between two curves, (green vertical dashes) Bragg positions (radiation Mo-Kα).

are also observed from $BaCuO_2$, $BaCO_3$, and CuO, as indicated in this figure. After heat treatment at 925 °C, the XRD results show that the wire sample with x = 0 presented a single phase (ICDD-JCPDS 64-642), while the compounds with Ni substitution of Cu atoms still presented additional reflections identified as belonging to the $BaCuO_2$ and CuO phases. Similar results can be observed in figure 3, which shows the x-ray diffraction patterns of samples with x = 0.00, 0.01, 0.02 and 0.04; all of the doped samples present low intense additional peaks of additional phases, similar to reports in the literature for similar compounds [4, 19].

To observe the influence of Ni substitution in $YBa_2Cu_{3-x}Ni_xO_{7-\delta}$ compounds, structural data were analyzed by the Rietveld method, using the FULLPROF crystallographic software [24]. Figure 4 displays the representative Rietveld refined XRD pattern for a YBCO nanowire sample heat-treated at 925 °C for 4 h in an oxygen atmosphere. The structural parameters derived from these analyses are listed in table 1. For the doped samples, we introduced the crystallographic data of the additional phase $BaCuO_2$ (ICDD-JCPDS 79-838). The Bragg factor (R_{Bragg}) and χ^2 values suggest that the simulated XRD pattern agrees well with the experimental XRD pattern.

These analyses show that the YBCO structure remains orthorhombic (space group symmetry *Pmmm*), and a small change in the lattice parameters can be observed with increasing Ni doping. The small change in *a*, *b* and *c* with x suggests that Ni replaces Cu in the crystallographic Wyckoff sites 1*a* and 2*q*, as predicted in the literature. This trend may also be associated with small ionic radius variations in Cu (0.57 Å) and Ni (0.55 Å) [25], which promote the formation of the superconducting orthorhombic structure in these samples. The lattice cell

Table 1. Structural data obtained for $YBa_2Cu_{3-x}Ni_xO_{7-\delta}$ (x = 0.01, 0.02 and 0.04) samples using Rietveld refinement. This table contains reliability factors (χ^2 and R_{Bragg}), volumetric fractions of the crystallographic phases identified as YBCO (V_{YBCO}), $BaCuO_2$ (V_{BaCuO_2}), and CuO (V_{CuO}) and the parameters *a*, *b* and *c* for these sample and from literature [11].

x	χ^2	R_{Bragg}	V_{YBCO}%	V_{BaCuO_2}%	V_{CuO}%	Volume (Å)	*a* (Å)	*b* (Å)	*c* (Å)
0	2.13	3.17	100(1)	—	—	171.99(2)	3.821 5	3.884 6	11.692 3
0.01	1.92	4.38	89.8(5)	7.3(3)	2.8(3)	172.25(2)	3.833 5	3.886 9	11.655 9
0.02	1.67	4.83	87.8(4)	9.2(3)	2.9(3)	172.43(3)	3.821 5	3.883 9	11.688 2
0.04	1.46	3.21	88.89(5)	10.7(2)	0.3(2)	172.43(4)	3.823 1	3.886 7	11.660 2
Literature	—	—	—	—	—	—	3.823 4	3.866 2	11.794 1

Table 2. Interatomic distances for $YBa_2Cu_{3-x}Ni_xO_{7-\delta}$.

x	Y−O	Ba−O	Cu_1−O	Cu_2−O	Ni_1−O	Ni_2−O
0	2.405(4)	2.843(3)	1.934(8)	1.991(4)	—	—
0.01	2.403(5)	2.849(4)	1.910(2)	2.005(8)	1.910(2)	2.005(8)
0.02	2.424(8)	2.838(6)	1.914(2)	1.999(8)	1.914(2)	1.999(8)
0.04	2.397(7)	2.853(5)	1.919(2)	2.002(3)	1.919(2)	2.002(3)

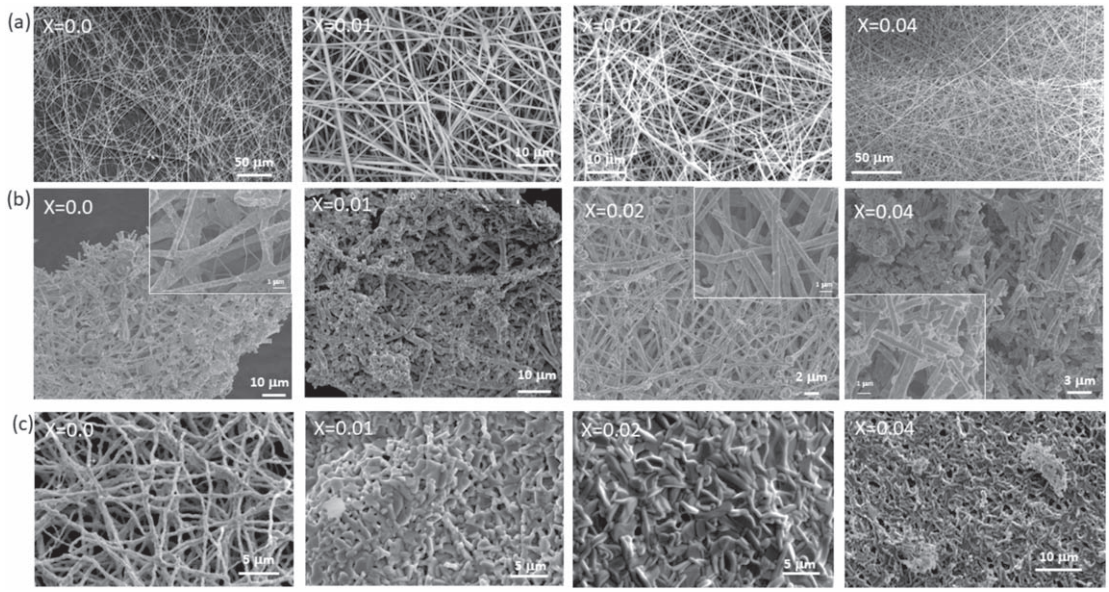

Figure 5. SEM images of $YBa_2Cu_{3-x}Ni_xO_{7-\delta}$: (a) dried at 100 °C (insets); and (b) heat-treated at 780 °C/10 h; and (c) 925 °C for 4 h in oxygen atmosphere.

parameters are close to those reported in the literature, the *a*, *b* and *c* values of the electrospun samples are slightly smaller than those found for bulk YBCO (see table 1) [11]. As a result, the unit cell volume V ∼ 172.0(1) Å calculated for the YBCO nanofibers is ∼1% smaller than the V ∼ 173.3(5) Å value observed for the bulk. Analyses of the lattice cell parameters for Ni-doped samples also revealed a increase in V values (table 1); these V values are slightly smaller than the results expected for similar bulk compounds. This last result can be related to the small crystallite size presented by these samples, ∼16.8 nm (estimated by the Scherrer relation) for sample x = 0.01 [26], due to the electrospinning process used to grow these samples. These subtle changes in the *a*, *b*, *c* and V values are primarily related to changes in the bond length of Cu_2−O_1 and the Cu_2−O−Cu_2 bond angle (see table 2), suggesting that Ni substitutes the Cu(2) in the plane, which is also in good agreement with results reported in the literature [14].

Figure 5 shows scanning electron microscopy (SEM) images of $YBa_2Cu_3O_{7-\delta}$ samples (a) after dried at 100 °C, (b) heat treated at 780 °C and (c) at 925 °C in an oxygen atmosphere. Figure 5(a) shows that all samples present a nanowire morphology when dried at 100 °C, with an external diameter ranging from 0.5 to 1.13 μm and a length >50 μm. As discussed above, we observed that all samples heat-treated at 780 °C for 10 h in oxygen atmosphere presented most of the desired crystalline phase, and in this condition all samples display a fibrous shape with a rough surface. Figure 5(b) shows the SEM images of these samples, which revealed ultrafine grains

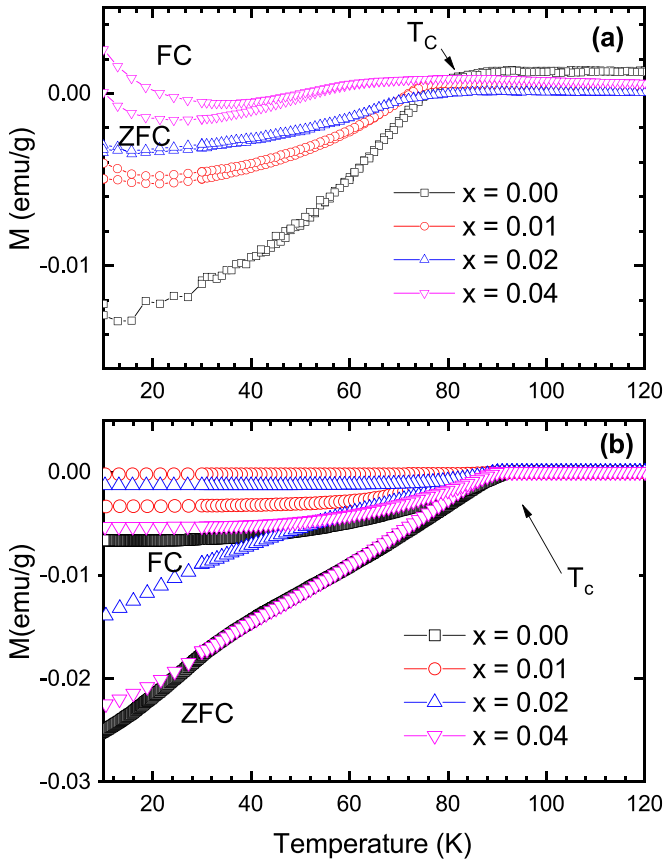

Figure 6. Magnetization as a function of temperature for $YBa_2Cu_{3-x}Ni_xO_{7-\delta}$ (x = 0.00, 0.01, 0.02 and 0.04) samples heat-treated at (a) 780 °C/10 h and (b) 925 °C/4 h in an oxygen atmosphere.

assembled in fibers with diameter ranging from 480 to 560 nm and length >10 μm. After heat treatment at 925 °C, only YBCO maintains its fibrous morphology, presenting a rough surface and long length; moreover, the nanofibers appear to coalesce with each other (see figure 5(c)). These nanofibers present external diameters varying from 400 to 500 nm and lengths greater than 10 μm. Previous studies on the synthesis of YBCO nanowires by electrospinning have reported nanowire diameters ranging from 400 to 600 nm [4, 19]. For the nickel-doped sample, this figure shows that the morphology changes drastically after heat treatment at 925 °C. In fact, the sample loses its fibrous-like shape, and the fibers appear to coalesce, forming aggregates that exhibit particles with a plate-like form for the samples with x = 0.01 and x = 0.02.

As high-T_c superconductors present an electronic structure with high anisotropy in the Cu−O planes, subtle changes in the structure can have a remarkable influence on the superconductivity of these systems [6]. To verify these results, all $YBa_2Cu_{3-x}Ni_xO_{7-\delta}$ ($0.00 \leqslant x \leqslant 0.04$) samples heat-treated at 780 °C/10 h and 925 °C/4 h in oxygen atmosphere were characterized by magnetization measurements, M(T). As previously discussed, Ni-doped samples heat-treated at 780 °C present a nanowire morphology, but only samples heat-treated for 10 h present superconductivity transitions. Figure 6(a) displays temperature-dependent magnetization curves for samples of $YBa_2Cu_{3-x}Ni_xO_{7-\delta}$ ($0.00 \leqslant x \leqslant 0.04$) heat-treated at 780 °C/10 h and 925 °C/4 h in an oxygen atmosphere (with an applied magnetic field of 100 Oe). All M(T) curves present a subtle decrease of the magnetization values below temperatures Tc that characterize a superconductor transition. The critical transition temperature, Tc, ranging from 93.2 K to 70 K to samples with x = 0 to x = 0.04, respectively, which is a little lower but close to values reported for similar samples and bulk in the literature [2, 27, 28]. Magnetic measurements of Ni-doped YBCO samples show that the superconductor transition width broadens with increasing substitutional Ni. This behavior can be interpreted as a distribution of transition temperatures due to an inhomogeneous distribution of Ni atoms or due to granular effects. Moreover, the T_c values decrease from 91.01K to 90.2 K for the samples with x = 0.01 and 0.04, respectively. This trend is in agreement with reports that the substitution of Cu by 3d elements results in a decrease of T_c in doped YBCO [14]. This behavior may also be related to structural variations resulting from the synthesis process, which reduced the volume of the unit cell and the Cu_2-O-Cu_2 bond angles. With the increase of the heat treatment temperature to 925 °C, the doped samples lost their nanowire shape, but all of them present a superconductor transition at Tc of 90.01 K to 92.6 K for the samples with x = 0.04 to 0.00, respectively. The M(T) magnitude also is larger than the samples heat-

treated at lower temperatures, which can be related with the size of the superconductor domains that is slightly larger for samples heat-treated at 925 °C.

4. Conclusions

Using x-ray diffraction analysis, it was verified that all of the samples crystallized in the desired crystalline phase; analysis also revealed the formation of the perovskite structure with orthorhombic symmetry (*Pmmm* symmetry group). However, the XRD results of the majority of samples present peaks of additional phases identified as CuO and $BaCuO_2$. It was found that the samples prepared by electrospinning presented lower a, b, and c values and a lower unit cell volume (V) compared to samples in the form of powder reported in the literature. From this study we observed that the morphology of the samples doped with nickel changes after heat treatment, and their nanowire morphology could be maintained if heat-treated at temperatures close to 780 °C for 10 h in an oxygen atmosphere. Magnetic characterization of the wire samples revealed the characteristic diamagnetic transition to superconducting at temperatures below T_c. For the doped samples, this value was near the T_c of 70 to 93.2 K, indicating that the substitution of Cu by Ni promoted a lower T_c. Thus, the magnetic characterization showed that the samples displayed behaviors similar to those reported in the literature.

Acknowledgments

The authors gratefully acknowledge the Multiuser Central Facilities at UFABC for experimental support (XRD, SEM, MPMS3-SQUID). The authors would like to acknowledge the UFSCAR-DQ for the magnetic measurements (MPMS3-SQUID—FAPESP no. 09/54082-2). Additionally, the authors acknowledge the financial support provided by CAPES, CNPq and FAPESP.

Conflict of Interest

The authors declare that they have no conflict of interest.

ORCID iDs

M T Escote https://orcid.org/0000-0003-1053-560X

References

[1] Muller K A and Bednorz J G 1987 The Discovery of a class of high-temperature superconductors *Science* **237** 1133–1139
[2] Wang W, Chen Q, Cui Qi, Ma Ji and Zhang H 2015 *Phys. C Supercond. Its Appl.* **511** 1
[3] Xu K and Heath J R 2008 *Nano Lett.* **8** 136–41
[4] Duarte E A, Rudawski N G, Quintero P A, Meisel M W and Nino J C 2014 *Superconductor Science and Technology* **28** 015006
[5] Duarte E A, Quintero P A, Meisel M W and Nino J C 2013 *Physica C* **495** 109–13
[6] Plakida N 2010 *High-Temperature Cuprate Superconductors: Experiment, Theory, and Applications* 166 (Berlin, Heidelberg: Springer Science & Business Media) (https://doi.org/10.1007/978-3-642-12633-8)
[7] Bar E, Levi D, Koren G, Shaulov A and Yeshurun Y 2014 *Physica C: Superconductivity and Its Applications* **506** 160–4
[8] Golubev D, Lombardi F and Bauch T 2014 *Physica C: Superconductivity and Its Applications* **506** 174–7
[9] Arpaia R, Golubev D, Baghdadi R, Arzeo M, Kunakova G, Charpentier S, Nawaz S, Lombardi F and Bauch T 2014 *Physica C: Superconductivity and Its Applications* **506** 165–8
[10] Palau A, Rouco V, Luccas R, Obradors X and Puig T 2014 *Physica C: Superconductivity and Its Applications* **506** 178–83
[11] Elsabawy K M 2011 *Cryogenics* **51** 452–9
[12] Alikhanzadeh-Arania S and Salavati-Niasari M 2012 *Journal of Nanostructures* **1** 62–68
[13] Busbee J, Biggers R, Kozlowski G, Maartense I, Jones J and Dempsey D 2000 *Eng. Appl. Artif. Intell.* **13** 589–96
[14] Westerholt K, Wüller H, Bach H and Stauche P 1989 *Phys. Rev.* B **39** 11680
[15] Bridges F, Boyce J, Claeson T, Geballe T and Tarascon J 1989 *Phys. Rev.* B **39** 11603
[16] Xu Y, Sabatini R, Moodenbaugh A, Zhu Y, Shyu S G, Suenaga M, Dennis K and McCallum R 1990 *Physica C* **169** 205–16
[17] Papari G, Carillo F, Stornaiuolo D, Massarotti D, Longobardi L, Beltram F and Tafuri F 2014 *Physica C: Superconductivity and Its Applications* **506** 188–94
[18] Litombe N E, Bollinger A, Hoffman J E and Božović I 2014 *Physica C: Superconductivity and Its Applications* **506** 169–73
[19] Cui X M, Lyoo W S, Son W K, Park D H, Choy J H, Lee T S and Park W H 2006 *Superconductor Science and Technology* **19** 1264
[20] Greenberg Y, Lumelsky Y, Silverstein M and Zussman E 2008 *J. Mater. Sci.* **43** 1664–8
[21] Niu C *et al* 2015 *Nat. Commun.* **6** 7402
[22] Ramaseshan R, Sundarrajan S, Jose R and Ramakrishna S 2007 *J. Appl. Phys.* **102** 7
[23] Cui X, Lyoo W, Son W, Park D, Choy J, Lee T and Park W 2006 *Supercond. Sci. Technol.* **19** 1264–8
[24] Rodriguez-Carvajal J 1990 *XV congress of the IUCr (Toulouse, France)* 127
[25] Shannon R D 1976 *Acta Crystallographica section A: Crystal Physics, Diffraction, Theoretical and General Crystallography* **32** 751–67
[26] Patterson A L 1939 *Phys. Rev.* **56** 978–82

[27] Keimer B, Kivelson S A, Norman M R, Uchida S and Zaanen J 2014 *Nature* **518** 179
[28] Dadras S and Ghavamipour M 2018 *Mater. Res. Express* **5** 016001